JGR Space Physics

RESEARCH ARTICLE
10.1029/2019JA026670

Pressure Gradients Driving Ion Transport in the Topside Martian Atmosphere

O. Hamil[1,2], T. E. Cravens[1], A. Rahmati[3], J. E. P. Connerney[4], and L. Andersson[5]

[1]Department of Physics and Astronomy, University of Kansas, Lawrence, KS, USA, [2]Department of Earth and Space Sciences, Georgia Institute of Technology, Atlanta, GA, USA, [3]Space Sciences Laboratory, University of California, Berkeley, CA, USA, [4]NASA Goddard Space Flight Center, Greenbelt, MD, USA, [5]Laboratory for Atmospheric and Space Physics, University of Colorado Boulder, Boulder, CO, USA

Key Points:
- Ions are driven from the subsolar point toward the dawn/dusk terminator modeled from large-scale MHD calculations using MAVEN data
- This study demonstrates that above about 300 km, the plasma motion should dominantly be driven by magnetic field pressure
- We demonstrate quantitative agreement of magnetic pressure versus solar zenith angle over most of the dayside between MGS and MAVEN

Correspondence to:
O. Hamil,
oliver.hamil@eas.gatech.edu

Citation:
Hamil, O., Cravens, T. E., Rahmati, A., Connerney, J. E. P., & Andersson, L. (2019). Pressure gradients driving ion transport in the topside Martian atmosphere. *Journal of Geophysical Research: Space Physics*, *124*, 6117–6126. https://doi.org/10.1029/2019JA026670

Received 28 FEB 2019
Accepted 22 JUN 2019
Accepted article online 4 JUL 2019
Published online 13 JUL 2019

Abstract Magnetic and thermal pressure gradient forces drive plasma flow in the topside ionosphere of Mars. Some of this flow can contribute to ion loss from the planet and thus affect atmospheric evolution. MAVEN measurements of the magnetic field, electron density, and electron temperature, taken over a 3-year time period, are used to obtain averaged magnetic and thermal pressures in the topside ionosphere versus altitude, solar zenith angle, and latitude. Magnetic pressures are several times greater than thermal pressures for altitudes greater than about 300 km; that is, the plasma beta is less than one. The total pressure increases with altitude in the ionosphere and decreases with increasing solar zenith angle. Using these pressure patterns in the dayside ionosphere to estimate the pressure gradient force in the fluid momentum equation, we estimate horizontal day-to-night plasma flow speeds of a few kilometers per second near 400 km.

1. Introduction

The structure of any planetary ionosphere is determined by a combination of chemical and dynamical processes. Plasma flows in response to the net force on a plasma fluid parcel (Cravens et al., 2017; Schunk & Nagy, 2009). The force balance on the ionospheric plasma at Mars is strongly affected by the solar wind interaction with that planet (Brain et al., 2015; Cravens et al., 2017; Ledvina et al., 2017; Ma et al., 2004, 2015). Solar wind dynamic pressure is converted mostly to thermal pressure at the bow shock and then into magnetic pressure in the magnetic pileup region (Crider et al., 2002; Ma et al., 2004). Magnetic pressure gradients in the topside ionosphere drive ion flow from day to night (Brain et al., 2015; Cravens et al., 2017; Crider et al., 2004). Thermal pressure gradients also drive day-to-night flow, largely mediated by the ambipolar electric field (Cravens et al., 2017; Ma et al., 2015). The topside ionospheric flow can contribute to ion loss from Mars (and thus atmospheric loss), under the right circumstances, and affect atmospheric evolution.

Day-to-night ion flow should lead to loss of O atoms in one of two ways (Cravens et al., 2017): (1) loss into the tail if the flow is at high enough altitudes or (2) if the flow is at low enough altitudes, possible fast atom escape (not as ions) via dissociative recombination of O_2^+ ions if the O_2^+ diffuses down on the nightside and/or O^+ ions diffuse down and react with CO_2 producing O_2^+. Some ion escape down the tail is observed, but tail data cannot indicate whether or not the ions came from the dayside or were produced locally on the nightside (e.g., via electron impact ionization; Brecht & Ledvina, 2012; Brain et al., 2015; Lundin et al., 2013; Nilsson et al., 2012).

MAVEN measurements of the magnetic field via the magnetometer instrument (MAG; Connerney et al., 2015) and of electron densities and temperatures with the Langmuir probe (LPW; Andersson et al., 2015), in the topside ionosphere are used to study the dynamics of plasma flow due to pressure gradients. The magnetic and thermal pressures varying with solar zenith angle, latitude, and altitude are studied using data from a 3-year time period, focusing on day-to-night flow. Cravens et al. (2017) described a simple procedure for empirically determining ion flow and loss using some MAVEN data, but for the magnetic pressure variations, mainly using averaged data from the Mars Global Surveyor (MGS) mission (Crider et al., 2004). In the current paper, we will advance beyond the Cravens et al. (2017) study by considering empirical magnetic and thermal pressure variations found using MAVEN data from a 3-year time period. We will then revisit the Cravens et al. (2017) conclusions with this new data. The implications for total ion loss from Mars will be discussed.

A recent paper by Wu et al. (2019) investigates ion flow using data from the MAVEN Neutral Gas and Ion Mass Spectrometer to determine the morphology of the topside ionosphere. In contrast, the current work uses data from LPW and MAG for determination of ion flow rates. The aspects of the two investigations should be considered complementary.

This paper is organized as follows: we give a brief review of the transport mechanism and claims in section 2, followed by the relevant graphs and compiled data in sections 3 and 4, followed by a discussion of the results and implications for ion loss in section 5, and a brief summary in section 6.

2. MHD Formalism

We briefly revisit equations from our recent paper (Cravens et al., 2017). The intent of the current work is to analyze MAVEN data, using simple theory, and compare to the previous results which incorporated MGS data. Establishing agreement between these data sets, connected to the simple magneto-hydrodynamics (MHD), is important to the study of the Martian atmosphere.

In Cravens et al. (2017), it is proposed that the transport of ion plasma in the topside ionosphere is the result of an MHD fluid force exerted on a plasma parcel. Further, it is assumed to be governed by the single-fluid momentum equation

$$\rho\left(\frac{\partial \mathbf{u}}{\partial t}+\mathbf{u}\cdot\nabla\mathbf{u}\right)=-\nabla(\mathrm{p}_e+p_i)+\mathbf{J}\times\mathbf{B}+\rho\mathbf{g}-\rho\nu_{\mathrm{in}}(\mathbf{u}-\mathbf{u}_n), \tag{1}$$

where ρ is the plasma mass density, $\mathbf{u}$ is the ion fluid velocity, p_e and p_i are the electron and ion pressures, $\mathbf{J}$ is the current density, $\mathbf{B}$ is the magnetic field vector, $\mathbf{g}$ is the acceleration due to gravity, ν_{in} is the ion-neutral momentum transfer collision frequency, and u_n is the neutral flow velocity.

Using Ampere's law and a few simplifying assumptions (see Cravens et al., 2017, for a complete derivation), we arrive at the simple model for a time-independent horizontal momentum

$$\frac{\mathrm{d}}{\mathrm{d}s}\left[\frac{1}{2}u^2+\frac{\mathrm{p}}{\rho}\right]+\nu_{\mathrm{in}}(u-u_n)=0 \tag{2}$$

in which the total pressure $\mathrm{p}=(p_e+p_i+p_B)$ is the sum of the thermal and magnetic pressures given by $\mathrm{p}_{e,i}=n_{e,i}k_BT_{e,i}$ and $\mathrm{p}_B=B^2/2\mu_0$, respectively, and it is assumed that ρ does not vary much over the horizontal distance, s.

Note that the magnetic force, J × B, includes both the magnetic pressure gradient force and a magnetic tension force, but in a simple analysis both forces scale as the magnetic pressure is divided by a length scale. We also assume that the gravitational term can be neglected for the horizontal day-to-night flow.

Ion flow rate should vary as a function of altitude and may be approximated under the various conditions in somewhat broadly defined yet distinct regions of altitude. High- and low-altitude approximations can be made in order to predict the related flow rates. For the purposes of this paper, we have defined these regions as being above and below about 600 km for high and low altitudes, respectively.

The simpler of these is the high-altitude approximation in which ion-neutral collisions can be neglected (i.e., $\nu_{\mathrm{in}}=0$). In this case,

$$\frac{1}{2}u^2+\frac{p}{\rho}=\text{constant}, \tag{3}$$

and the flow speed is approximated as the subsolar Alfven speed (see Cravens et al., 2017, for detailed discussion).

The low-altitude approximation is of particular importance to the current work because it predicts the expected horizontal flow due to magnetic pressure gradients that we expect to see in MAVEN observations. Using equation (2) and assuming u^2 is small (Cravens et al., 2017), we have the low-altitude equation of ion flow relative to the neutral speed,

$$u-u_n=-\frac{1}{\rho\nu_{\mathrm{in}}}\frac{\mathrm{d}p}{\mathrm{d}s}. \tag{4}$$

From equation (4), it is clear that the ion flow, relative to the neutral speed, varies proportionally with the horizontal plasma pressure gradient and inversely to the ion-neutral collision frequency. Assuming that

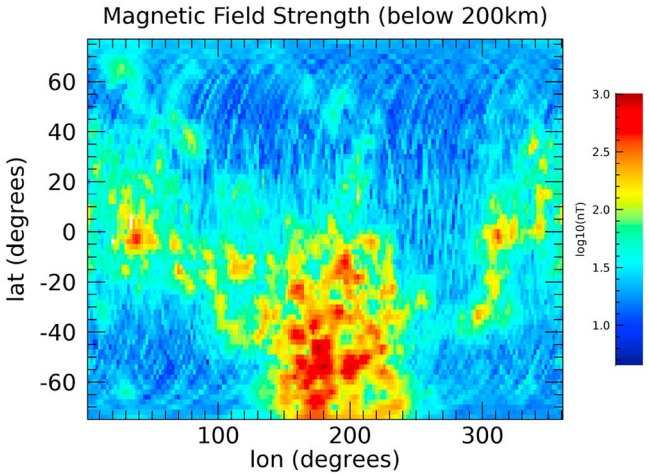

Figure 1. Crustal field plotted in units of nanotesla and binned by latitude and longitude at Mars. We see the significant difference in crustal magnetic field occurrence, as denoted by the dark red regions on the map, between the northern and southern hemispheres.

the plasma pressure gradient decreases from the subsolar point toward the terminator, we should see flow toward the nightside of the planet. Moreover, as the ion-neutral collision frequency increases with increased neutral density, as with lower altitudes, we expect to see a gradient in flow speed as a function of altitude for a given solarzenith angle (SZA). Indeed, we expect ion flow to be slowed via its inverse proportionality to ion-neutral collision frequency.

Cravens et al. (2017) use reasonable assumptions for the pressure gradient dp/ds and the collision frequency ν_{in} in order to determine flow speeds as a function of solar zenith angle at a given relevant altitude. In this case, ds is related to SZA via $ds = rd\chi$, where r is the total radius defined as the Mars radius R_m plus altitude z and χ is the SZA. We will inspect 3 years of MAVEN data to compare with the conclusions of the previous work.

3. MAVEN Data Analysis

We use averaged data from a 3-year period of the MAVEN mission starting 1 January 2015 and ending at 1 January 2018. We exclude the most recent data in order to ensure consistency in the data quality. All relevant observations are plotted and explained in terms of their relevance to our analytical predictions from Cravens et al. (2017).

We are interested in transport due to ionospheric pressures mainly associated with the solar wind interaction and therefore seek to exclude effects coming from the crustal fields. We therefore separate data for the northern and southern hemispheres in order to account for crustal magnetic field dominance in the southern hemisphere and mitigate its significance in our results.

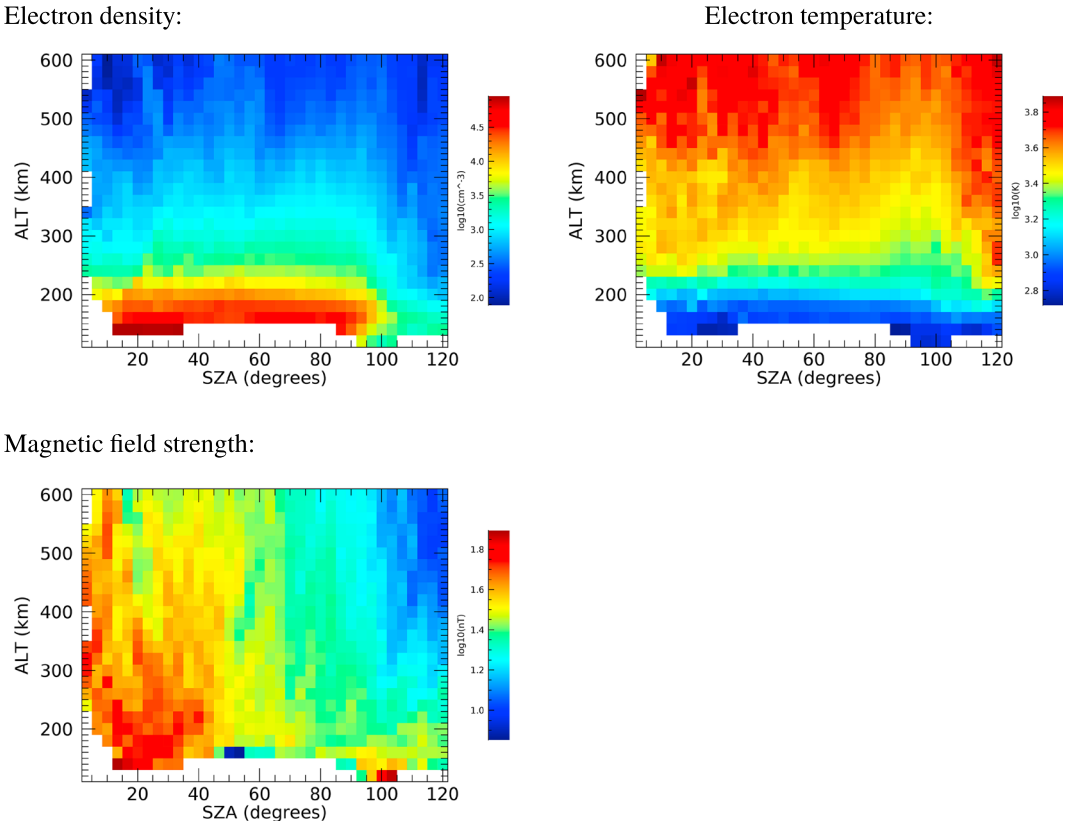

Figure 2. Averaged values binned in altitude and solar zenith angle for the northern hemisphere. SZA = solar zenith angle.

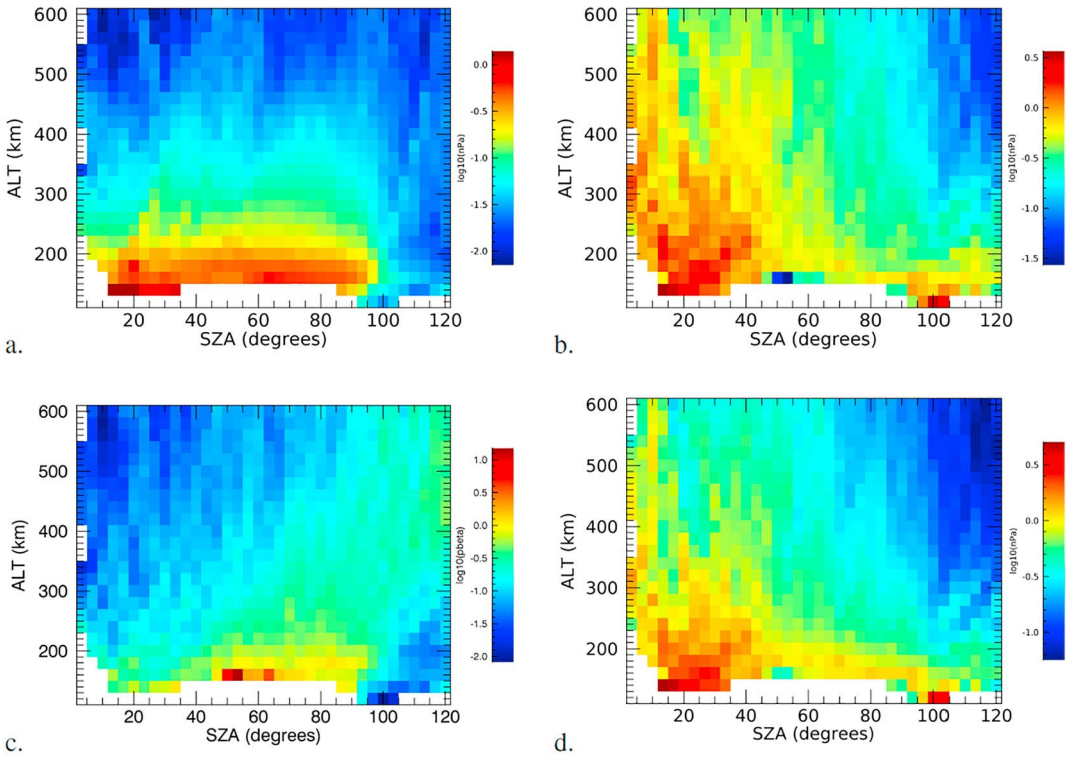

Figure 3. Averaged pressures binned in altitude and solar zenith angle for the northern hemisphere. (a) Combined electron and ion thermal pressure. (b) Magnetic pressure. (c) Plasma beta. (d) Total pressure ($P_B + P_{thrm}$). SZA = solar zenith angle.

Figure 1 shows the prevalence of crustal fields on a planetary scale. We see the relative dominance of these fields in the southern hemisphere. In order to reduce or identify the interference of crustal effects in the data, we investigate the northern and southern hemispheres separately. In order to reduce crustal interference, we focus our topside ion flow investigation in the northern hemisphere where we assume that the crustal effects are lower when compared to the southern hemisphere due to the discrepancy in crustal field prevalence shown in Figure 1. We note here that this is a crude assumption given that other authors have shown that crustal fields can affect plasma flow in both hemispheres. For instance, Xu et al. (2017) determined, using MAVEN electron data, that the plasma is connected to crustal fields as well as the solar wind. We do not claim to eliminate crustal effects; however, the difference in magnetic pressure profiles between the northern and southern hemispheres will indicate larger crustal field effects in the southern hemisphere due to, as shown in Figure 1, a larger concentration of crustal fields in the southern hemisphere. As will be discussed later, we see agreement with our analytical results in the southern hemisphere as well but at higher altitudes. We make no detailed conclusions about the crustal fields themselves, but this could be done in future work.

4. Empirical Thermal and Magnetic Pressure Patterns

In this section, we show magnetic field data, magnetic pressures, and thermal pressures versus solar zenith angle and altitude, separated into the northern hemisphere (section 4.1) and southern hemisphere (section 4.2).

4.1. Northern Hemisphere

Observations in the northern hemisphere are less affected by crustal magnetic fields, particularly at higher altitudes.

Figure 2 shows the variables required to determine the pressure gradients relevant to our study. We show averaged values from 3 years of MAVEN data coming from the MAG and LPW instruments. From these data, we are able to calculate the magnetic and thermal pressures. The thermal pressure is estimated from the electron density and temperature. We see from the plots that there is not a clear gradient in either electron

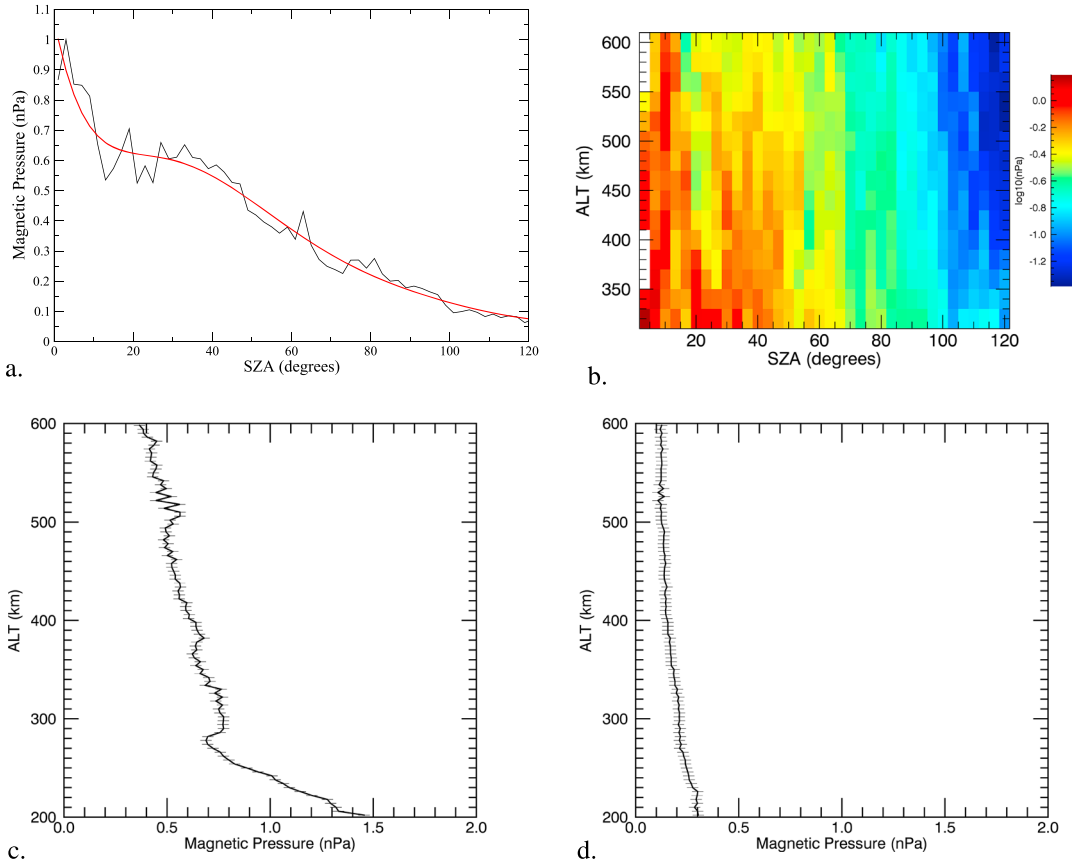

Figure 4. Magnetic pressure averages in the northern hemisphere below 600-km altitude. (a) Line plot of average magnetic pressure as a function of SZA in the range of roughly 300–600 km. (b) Average magnetic field displayed in altitude and SZA. (c) Altitude profile of average magnetic pressure across 30–40° SZA (dayside). (d) Altitude profile of average magnetic field strength across 90–100° SZA (terminator). SZA = solar zenith angle.

density or pressure as a function of solar zenith angle. Unremarkably, we see a clear altitude dependence on both quantities. As would be expected in this system, the electron density (temperature) is higher (lower) at low altitudes and decreases (increases) with increasing altitude.

Conversely, from Figure 2, we see a clear gradient in magnetic field over SZA in the range of altitude (i.e., 250–450 km roughly). For this altitude range, the magnetic field strength varies from about 40 nT down to about 15 nT, or lower, from the subsolar point toward the nightside of the planet.

From the data in Figure 2, we can calculate the magnetic and thermal pressures which drive the plasma flow. The magnetic pressure is given by $P_B = B^2/2\mu_0$ which is read directly from the MAG data in the figure. The total thermal pressure is given by $P_{thrm} = k_B(nT_{electron} + nT_{ion})$, where we estimate the ion density to equal the LPW measured electron density by imposing charge neutrality. It is reasonable to assume that the electron temperatures are roughly twice the ion temperatures (Chen et al., 1978; Sakai et al., 2016). We therefore calculate the total temperature as $T = 1.5T_e$.

The calculated pressures are shown in Figure 3. We see the relative dominance of magnetic pressures over thermal pressures by inspection. The plot of plasma β confirms magnetic pressure dominance and also reaffirms the gradient across solar zenith angle. Finally, we show, in the lower right panel of Figure 3, the total pressure which is due mainly to magnetic pressure.

In Figure 4, we show the magnetic pressure in the relevant region of altitude and SZA. The magnetic pressure gradient, assumed responsible for transporting ions from day to night, shows a clear gradient across increasing SZA in the top plots. In the lower figures, we see the difference in the altitude profiles on the dayside and across the terminator.

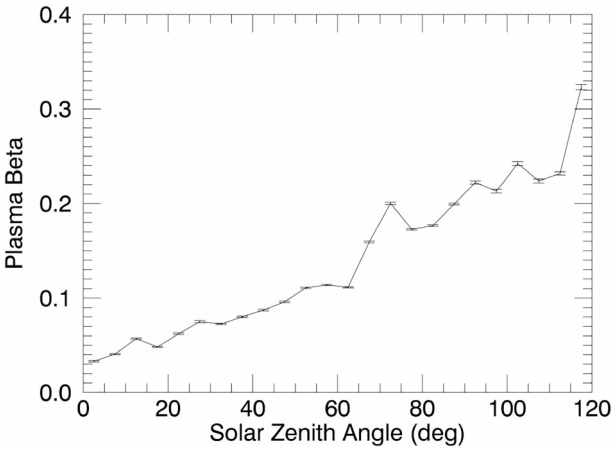

Figure 5. Plasma beta as a function of solar zenith angle. The line represents all data in the 3-year range averaged over 300–600 km in altitude.

The plasma beta, averaged over 300–600 km, is significantly less than unity (Figure 5) for all solar zenith angles on the dayside. Note that this does not mean that beta is not greater than one on some orbits or during certain circumstances. Past the terminator, on the near nightside, the plasma beta becomes close to one. This result indicates that, on average, magnetic forces are more important than pressure forces (including the ambipolar electric field effect which mainly manifests itself as an electron pressure gradient force) in driving day-to-night topside ionosphere flow. Also note that for directions parallel to the magnetic field, the thermal pressure gradient term is very important but the flow speeds generated by the pressure gradients will be less than the speeds generated by the magnetic field for directions perpendicular to the magnetic field.

We compare our results with previous results calculated from the magnetic field data from the MGS (Crider et al., 2003) as shown in Figure 6. The good agreement indicates that (1) at least the magnetic force part of the day-to-night ionospheric dynamics is most likely similar for the MGS and MAVEN epochs and (2) the Cravens et al. (2017) ion loss analysis, which used MGS magnetic data, also applies to the MAVEN epoch. We

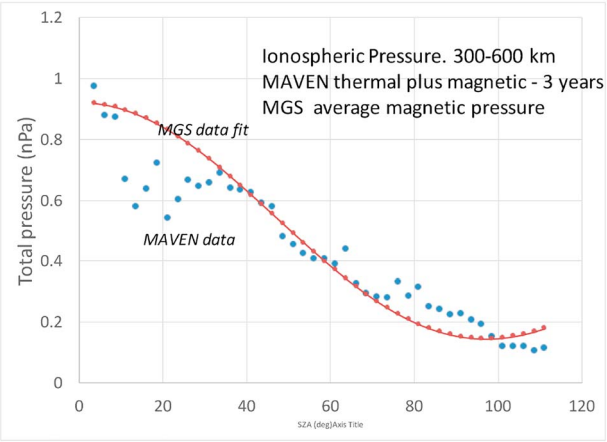

Figure 6. MAVEN data averaged over 3 years of observation are compared with that fitted to MGS (Cravens et al., 2017). We see good agreement between the two data sets which show total pressure (magnetic + thermal) as a function of solar zenith angle in MSO coordinate space. It should be noted here that this comparison includes thermal pressure from MAVEN (absent from MGS). We are interested in total pressure, which drives the dynamics, but due to the low plasma beta, we see good agreement with the MGS estimated pressure due only to magnetic field data. MGS = Mars Global Surveyor.

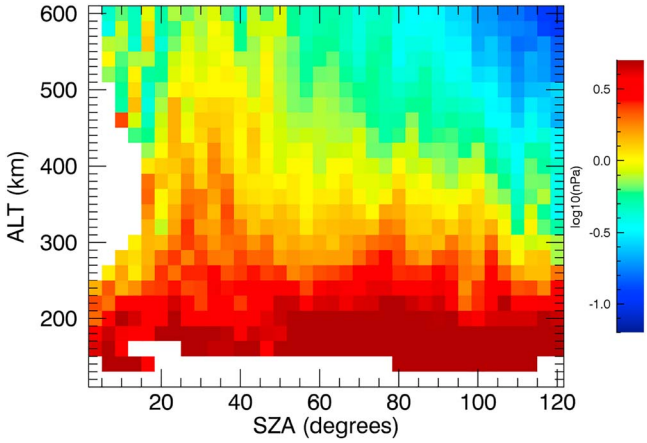

Figure 7. Average total pressure (thermal + magnetic) values binned in altitude and solar zenith angle for the southern hemisphere. SZA = solar zenith angle.

note the apparent discrepancy in agreement occurring near 20° SZA. The amount of MAVEN data available at very low SZA was limited, and selection effects result in this variation in the two data sets.

4.2. Southern Hemisphere

We will briefly discuss the southern hemisphere observations, in comparison with the North, to estimate the differences due to the crustal fields. As seen in Figure 1, the crustal magnetic field is significantly more prevalent in the southern hemisphere and is seen strongly in the magnetic field data below 200–250 km, which skews the description of ion flow. In order to mitigate this effect, as previously discussed, we separated the planet into two hemispheres by latitude. In the southern hemisphere data, a less well defined magnetic pressure gradient (due to crustal fields) is evident at lower altitudes. The differences in the north and south can be attributed to crustal field contributions as seen in Figure 1, and to the extent that it may be determined with more certainty should be left to future work.

In Figure 7, we see a small gradient in total pressure but not as clearly defined, or as powerful, as we see in the northern hemisphere. This is due to the large presence of the remnant crustal magnetic field which spreads fairly evenly across the averaged solar zenith angle up to about 300 km. Above 300 km, we see the manifestation of a pressure gradient similar (albeit less intense) to that of the northern hemisphere.

We see no distinct horizontal magnetic pressure gradient below 300 km in the southern hemisphere. In fact, we see a large fluctuation due to the crustal fields in that region. In the higher altitudes, we see a gradient

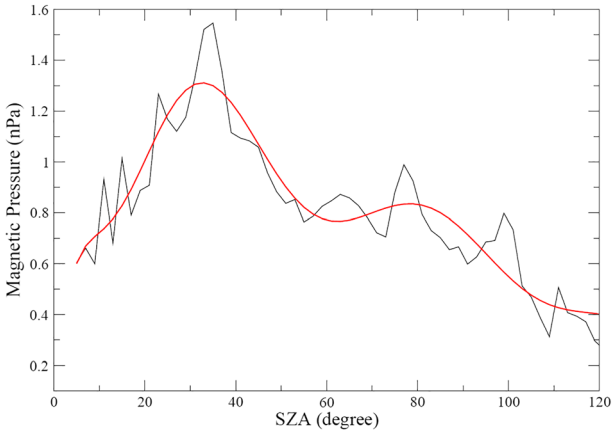

Figure 8. Total averaged southern hemisphere magnetic pressure as a function of solar zenith angle. Altitude range: 300–600 km. We see indication of crustal interference across solar zenith angle. We see signs of a pressure gradient similar to what is seen in the north after about 40° SZA; however, the interference from crustal fields is well illustrated by the noise in this figure. SZA = solar zenith angle.

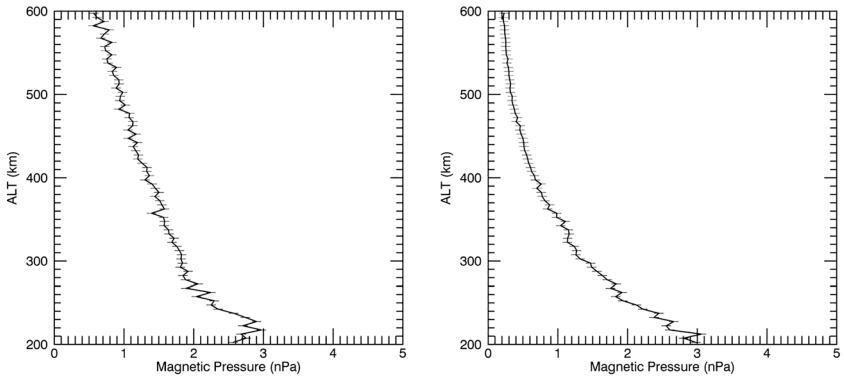

Figure 9. Altitude profiles of magnetic pressure averaged over the indicated range of solar zenith angle in the southern hemisphere. The plots show a pattern of crustal interference where the magnetic field somewhat steadily increases with lower altitude. We do not see the same pattern of a peak in the magnetic pileup region as is seen in the northern hemisphere data. (left) SZA range: 30–40°. (right) SZA range: 90–100°.

trend across SZA, as shown in Figure 8, but not as clearly as seen in the northern hemisphere. We also note the lower variation in pressure (nPa).

In the averaged southern hemisphere altitude profiles shown in Figure 9, we do not see a clear magnetic pileup region. Instead, we find a gradual curve increasing with decreased altitude on the dayside and a similar behavior at the terminator with an added large spike at very low altitudes. Both the increase in average field strength and the large spike can be attributed to crustal field interference.

To illustrate the significance of crustal field interference in the magnetic field pressures, we examine Figures 8 and 9.

5. Discussion: Plasma Flow Speeds

In our study, we are focused on the dominant day-to-night ion flow associated with horizontal gradients driving plasma from low to high solar zenith angle. There may be other pressure gradients in the system driving ion flow, for example, from the southern hemisphere to the northern hemisphere. While likely present, these flows are complicated to predict, and since we are concerned mostly with flows toward the nightside, we leave the possible hemispheric pressure gradients to future work.

The bottom plots in Figure 4 and the plots in Figure 9 show the vertical profile of averaged magnetic pressures for the northern and southern hemispheres, respectively. The two plots for each hemisphere represent averages extending positively near the dayside subsolar position (30–40 sza) and over the terminator (90–100 sza). For each hemisphere, comparison of these profiles illustrates the relative pressure values for these two representative positions. It is clear that, for the northern hemisphere, there is an average difference of about 0.45 nPa at the 300- to 400-km altitude favoring the dayside values. We also see a peak in pressure just below about 300 km on the dayside that is not present at the terminator. Looking at the same plots for the southern hemisphere, we see a similar average pressure gradient in the 300- to 400-km range, but the structure of the pressure profile is unchanged from the dayside to the terminator. One may speculate that this is the effect of strong crustal field interference, but this is beyond the scope of the current work.

It may also be noted that when these profiles are compared directly between southern and northern hemispheres, one sees a clear pressure increase in the south. One may also speculate that this represents a pressure gradient from the southern hemisphere to the northern hemisphere at both the subsolar point and at the terminator. In our estimation, this is a clear effect of the relative dominant presence of crustal fields in the south versus the north. This is further indicated by noting that the gradient at low altitudes is much greater than at high altitudes when comparing the northern and southern hemispheres. In the current work, we do not seek to describe the morphology of crustal fields or predict ion flow from low altitudes between the hemispheres. Rather, we are interested in ion flow from dayside to the nightside in general. The determination of ion flow along pressures associated with crustal fields is an important topic but beyond the scope of this work.

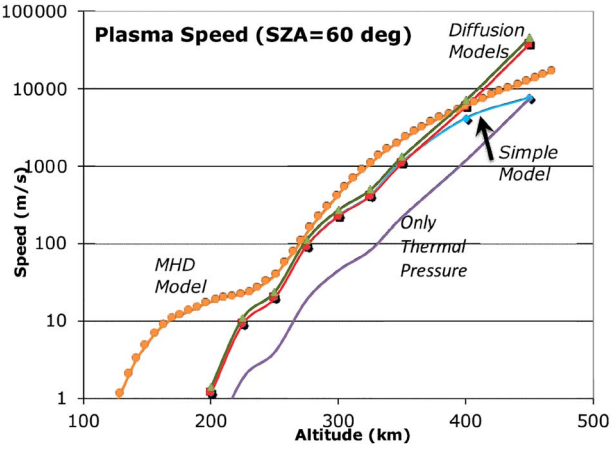

Figure 10. This figure is adapted from Cravens et al. (2017). Empirical pressure gradients (MAVEN) are used to estimate the ionospheric horizontal flow speed versus altitude at a solar zenith angle of 60°. One curve is generic dayside speed from the Ma et al. (2004) MHD model. One curve is from an analytical dynamical expression (labeled "simple model") using the empirical forcing. And the other three curves are estimated speeds using an ambipolar diffusion approximation. The bottom one (labeled "only thermal pressure") adopts a thermal pressure variation that is 20% of the magnetic variation derived in this paper (based on typical plasma beta). The next highest is just for magnetic pressure, and the top diffusion case includes both thermal and magnetic pressures. SZA = solar zenith angle.

The thermal and magnetic pressure derived from MAVEN data versus altitude and solar zenith angle indicate a day-to-night pressure gradient force on the ionospheric plasma that should drive plasma flow. The ion flow velocities (and ion escape rates) derived by Cravens et al. (2017), using MGS magnetic pressure variations and MAVEN data for plasma and neutral densities, should remain valid given that the current paper demonstrates that the pressure variations with SZA, at least for altitudes near 400 km derived from MAVEN data, are consistent with the MGS results.

Figure 10, adapted from Cravens et al. (2017), shows the speed versus altitude for a solar zenith angle of 60°. One simple model curve is for purely magnetic forces. The speed of day-to-night thermal pressure forces is included and is very roughly estimated by enhancing the other curve by 20% (i.e., the daytime plasma beta near 300–400 km). We did a similarly very simple estimate of plasma flow due to pure thermal pressure effects (i.e., this could be expected for flow parallel to the magnetic field) by taking 20% of the original speed. Not surprisingly, in all cases, the speed increases with altitude due to lower ion-neutral collision frequencies. Note that the plasma should flow at the same velocity as the neutral gas at lower altitudes where the ion-neutral collision frequency is very high (below about 250–300 km according to Cravens et al., 2017), but we do not show this here.

Measuring plasma flow velocities in the ionosphere is difficult because these velocities are small, or comparable to the spacecraft speed, and because the measurements are sensitive to spacecraft potential. We hope in the future to use MAVEN Supra Thermal and Thermal Ion Composition data to find the parameters of ionospheric O^+ and O_2^+ flow and see how these conform to our simple model.

6. Conclusions and Summary

We compiled 3 years of MAVEN data in order to investigate pressure-driven ion flow in the Martian upper atmosphere. We see relative dominance by magnetic field pressure, especially on the dayside, which drives ion flow from the subsolar point toward the terminator. This is in agreement with the findings of Cravens et. al (2017) in which ion flow was predicted via a simple MHD approach. We have added an analysis of MAVEN data using the same simple MHD approach and have found consistency in the results, which is a consequence of agreement between measured magnetic field data from the MAVEN and MGS missions.

The pressure gradients calculated from MAVEN magnetometer (Connerney et al., 2015) and LPW (Andersson et al., 2015) instrument observations show the expected flow speed variations as functions of altitude and solar zenith angle. Ion flow rates increase with increasing altitude due to reduced neutral density, and may be expected to follow a horizontal gradient, perpendicular to the magnetic field. The first of these observations is clear from physical principles and confirms the consistency of the MAVEN data. The horizontal magnetic pressure gradient is consistent with the findings of Cravens et al. (2017) and shows agreement with the MGS magnetic field data. We can reasonably expect a horizontal flow pattern indicated by the pressure gradient.

Acknowledgments
MAVEN data are available in the Planetary Data System (http://ppi.pds.nasa.gov/mission/MAVEN). This work was supported at the University of Kansas by NASA Grant NNH10CC04C to the University of Colorado and by subcontract to the University of Kansas. The MAVEN project is supported by NASA through the Mars Exploration Program.

References

Andersson, L., Ergun, R. E., Delroy, G. T., Eriksson, A., Westfall, J., Reed, H., et al. (2015). The Langmuir Probe and Waves (LPW) instrument for MAVEN. *Space Science Reviews*, *195*, 173–198. https://doi.org/10.1007/s11214-015-0194-3

Brain, D. A., McFadden, J. P., Halekas, J. S., Connerney, J. E. P., Bougher, S. W., Curry, S., & Seki, K. (2015). The spatial distribution of planetary ion fluxes near Mars observed by MAVEN. *Geophysical Research Letters*, *42*, 9142–9148. https://doi.org/10.1002/2015GL065293

Brecht, S. H., & Ledvina, S. A. (2012). Control of ion loss from Mars during solar minimum. *Earth, Planets and Space*, *64*, 165–178. https://doi.org/10.5047/eps.2011.05.037

Chen, R. H., Cravens, T. E., & Nagy, A. F. (1978). The Martian ionosphere in light of the Viking observations. *Journal of Geophysical Research*, *83*, 3871–3876. https://doi.org/10.1029/JA083iA08p03871

Connerney, J. E. P., Espley, J., Lawton, P., Murphy, S., Odom, R., Oliversen, R., & Sheppard, D. (2015). The MAVEN magnetic field investigation. *Space Science Reviews*, *195*, 257–291. https://doi.org/10.1007/s11214-015-0169-4

Cravens, T. E., Hamil, O., Houston, S., Bougher, S., Ma, Y., Brain, D., & Ledvina, S. (2017). Estimates of ionospheric transport and ion loss at Mars. *Journal of Geophysical Reseach: Space Physics*, *122*, 10,626–10,637. https://doi.org/10.1002/2017JA024582

Cravens, T. E., Rahmati, A., Fox, J. L., Lillis, R., Bougher, S., Luhmann, J., & Jakosky, B. (2017). Hot oxygen escape from Mars: Simple scaling with solar EUV irradiance. *Journal of Geophysical Research: Space Physics*, *122*, 1102–1116. https://doi.org/10.1002/2016JA023461

Crider, D. H., Acuna, M. H., Connerney, J. E. P., Vignes, D., Ness, N. F., Krymskii, A. M., & Winterhalter, D. (2002). Observations of the latitude dependence of the location of the Martian magnetic pileup boundary. *Geophysical Research Letters*, *29*(8), 1170. https://doi.org/10.1029/2001GL013860

Crider, D. H., Brain, D. A., & Acuña, M. H. (2004). Mars Global Surveyor observations of solar wind magnetic field draping Around Mars. *Space Science Reviews*, *111*, 203–221. https://doi.org/10.1023/B:SPAC.0000032714.66124.4e

Crider, D. H., Vignes, D., Krymskii, A. M., Breus, T. K., Ness, N. F., Mitchell, D. L., et al. (2003). A proxy for determining solar wind pressure at Mars using Mars Global Surveyor data. *Journal of Geophysical Research*, *108*(A12), 1461. https://doi.org/10.1029/2003JA009875

Ledvina, S. A., Brecht, S. H., Brain, D. A., & Jakosky, B. M. (2017). Ion escape rates from Mars: Results from hybrid simulations compared to MAVEN observations. *Journal of Geophysical Research: Space Physics*, *122*, 8391–8408. https://doi.org/10.1002/2016JA023521

Lundin, R., Barabash, S., Holmström, M., Nilsson, H., Futaana, Y., Ramstad, R., et al. (2013). Solar cycle effects on the ion escape from Mars. *Geophysical Reseach Letters*, *40*, 6028–6032. https://doi.org/10.1002/2013GL058154

Ma, Y., Nagy, A. F., Sokolov, I. V., & Hansen, K. C. (2004). Three-dimensional, multispecies, high spatial resolution MHD studies of the solar wind interaction with Mars. *Journal of Geophysical Research*, *109*, A07211. https://doi.org/10.1029/2003JA010367

Ma, Y. J., Russell, C. T., Fang, X., Dong, Y., Nagy, A. F., Toth, G., & Jakosky, B. M. (2015). MHD model results of solar wind interaction with Mars and comparison with MAVEN plasma observations. *Geophysical Research Letters*, *42*, 9113–9120. https://doi.org/10.1002/2015GL065218

Nilsson, H., Stenberg Wieser, G., Futaana, Y., Holmström, M., Barabash, S., Lundin, R., et al. (2012). Ion distributions in the vicinity of Mars: Signatures of heating and acceleration processes. *Earth Plantes Space*, *64*, 135–148. https://doi.org/10.5047/eps.2011.04.011

Sakai, S., Andersson, L., Cravens, T. E., Mitchell, D. L., Mazelle, C., Rahmati, A., et al. (2016). Electron energetics in the Martian dayside ionosphere: Model comparisons with MAVEN data. *Journal of Geophysical Research: Space Physics*, *121*, 7049–7066. https://doi.org/10.1002/2016JA022782

Schunk, R. W., & Nagy, A. F. (2009). *Ionospheres: Physics, plasma physics and chemistry* (2nd Ed.). UK: Cambridge University Press.

Wu, X. S., Cui, J., Xu, S. S., Lillis, R. J., Yelle, R. V., Edberg, N. J., et al. (2019). The morphology of the topside Martian ionosphere: Implications on bulk ion flow. *Journal of Geophysical Research: Planets*, *124*, 734–751. https://doi.org/10.1029/2018JE005895

Xu, S., Mitchell, D., Xiaohua, F., Yingjuan, M., Luhmann, J., Brain, D., et al. (2017). Martian low-altitude magnetic topology deduced from MAVEN/SWEA observations. *Journal of Geophysical Research: Space Physics*, *122*, 1831–1852. https://doi.org/10.1002/2016JA023467